Transactions, SMiRT-25
Charlotte, NC, USA, August 4-9, 2019
Division V

Experimental Study on Initial Stiffness Degradation and Its Effect on Seismic Capacity of Shear Wall with High Reinforcement Volume
Part 2: Static Loading Test on Effect of Damage on Seismic Performance

Jingyue SUN [1], AHMAD GHAZI ALJUHMANI[1] , Hamood ALWASHALI[2], Masaki MAEDA[3], Kiyoshi HIROTANI[4],Yoshihiro OGATA[5], Naoyuki AIZAWA[6], Masayasu KUSAKA[7]

[1] Graduate Student, Department of Architecture and Building Science, Tohoku University, Japan
[2] Assistant Professor, Department of Architecture and Building Science, Tohoku University, Japan
[3] Professor, Department of Architecture and Building Science, Tohoku University, Japan
[4] General Manager, Civil & Architectural Engineering Dept., Tohoku Electric Power Co., Japan
[5] Deputy General Manager, Civil & Architectural Engineering Dept., Tohoku Electric Power Co., Japan
[6] Specialty Leader, Civil & Architectural Engineering Dept., Tohoku Electric Power Co., Japan
[7] Civil & Architectural Engineering Dept., Tohoku Electric Power Co.,Inc., Japan

ABSTRACT

The Great East Japan Earthquake occurred on March 11, 2011 with magnitude of Mw 9, caused different levels of damage throughout the Tohoku region. The seismic response for the Nuclear Reactor Building of Unit 2 of the Onagawa NPP remained within elastic range, although hairline cracks were observed in shear walls. The slightly damaged walls in the reactors are thought not to affect the safety of the reactor due to the high safety factors used in the design of RC walls. However, the degradation of seismic capacity of shear walls due to previous slight damage is still unclear. The objective of Part 2 of this study is to clearly quantify the degradation of seismic capacity at each of the classified damage state based on experimental results of static cyclic loading tests of shear walls.

3 series of tests were conducted with each series having 4 specimens of 1\4 scale reinforced concrete (RC) shear wall. The investigated parameters are: two ratios of wall reinforcement, column and flanged boundary of shear wall and four levels of initial damage. The specimens were designed to fail in shear to represent a concrete shear walls in reactor buildings. The seismic capacity was investigated based on the influence of the prior damage on stiffness degradation, ultimate strength, deformation capacity, and energy dissipation.

The results showed that no significant deterioration was observed in ultimate strength and maximum deformation capacity due to previous damage. RC walls having boundary elements as flange walls had relatively greater stiffness degradation due to prior damage. The relationship between prior damage level and observed degradation of stiffness is investigated carefully. Such relationship is of great interest for modelling damaged RC walls due to a previous earthquake and estimate its seismic response based on modified backbone curve.

1. Introduction

The recent understanding of ground motion demands of earthquakes and advancement in seismic design allowed us to build structures that will perform well with limited damage after an earthquake. This reduced the number of severely damaged structures that need to be demolished after an earthquake. However, that also increased the number of structures with light and moderate damage. Those slightly damaged structures need to be evaluated again to get to know whether they will stand another earthquake or not, and what is the performance expected after such damage. In other words, how much is the residual seismic capacity. Several experiments were conducted to investigate the influence of prior damage and prior loading on the

seismic performance of RC columns such as (Pujol et al. 2006) and for beams (Marder et al. 2018). However, experiments to investigate the residual seismic capacity of RC walls due to previous damage is still limited. One example is the Nuclear Reactor Building of Unit 2 of the Onagawa NPP which experienced an earthquake of Magnitude 9, during Great East Japan Earthquake, on March 11, 2011. The nuclear reactor building of Unit 2 of the Onagawa NPP performed well and remained within elastic range, but slight cracks were observed in shear walls. The influence of this very slight damage on the safety are thought not to be of a great concern due to the high safety factors in design of RC walls of the reactor. However, the degradation of seismic performance needs to be clearly evaluated and this is the main motivation and purpose of this study. There are no previous studies stating and experimenting such influence on shear walls.

The purpose of this paper is to investigate the influence of pre-damage levels on the ultimate state performances, such as stiffness, shear strength, deformation and energy dissipation capacity, by conducting static cyclic loading tests of reinforced concrete shear walls. In other words, the RC walls were first loaded until it experienced a certain damage level, then reloaded again until its failure. 3 Series of tests were conducted with each series represents a certain parameter. Each series have 4 specimens of 1\4 scale reinforced concrete (RC) shear wall. The investigated parameters are: two levels of wall reinforcement ratio, influence of boundary elements at ends of shear wall. Also, four levels of initial damage which are identified based on the Japanese Post Seismic Evaluation Standard (JBDPA 2015) were investigated. The specimens were designed to fail in shear to represent a concrete shear walls in reactor buildings.

2. Experimental Plan

2.1 Outline of Experiment

Three different series of tests were conducted (SC-13, SC-06, SF-13); each one comprised of 4 identical specimens of reinforced concrete shear walls. All of the walls were designed to be shear critical, and with a scale factor of 1:4 of the original shear walls of nuclear power plants.

The parameters taken into consideration were damage level (before conducting the main test), reinforcement ratio in the shear wall, and the boundary elements of the shear walls. More specifically, SC-13 represents walls with lateral reinforcement ratio of 1.3% and with columns as boundary elements (S represent shear wall, C indicates that columns are boundary elements of the wall and the number 13 represent lateral reinforcement ratio of 1.3%). Series SC-06 are shear walls with lateral reinforcement ratio of 0.6% and columns as boundary elements. Series SF-13 have shear walls with the same amount of reinforcement as SC-13 Series, but with Flange walls as boundary elements. In other words, SC-13 Series and SC-06 Series have exactly the same boundary elements which are columns but with different reinforcement ratio, whereas in SF-13 Series flange walls were used as boundary elements.

Specimens named as (0) in each series represents the undamaged wall which was tested without pre-loading to obtain the capacity of the original shear wall which are the control specimens to which damaged walls will be compared. The test parameter for each series is different damage levels induced to each specimen (S-DI, II, III, IV) by a preloading. After the pre-loading phase main loading is to be conducted. The damage level is used as described in the Japanese Standard (JBDPA 2015). The description and judgment of damage levels will be described in later section of this study.

Note that specimens SC-13-DII, SC-06-DII and SF-13-DI were reused as specimen SC-13-DIV, SC-06- DIV and SF-13-DIV, respectively. This is because the damage of these specimens was quite limited and the deterioration of the capacity by pre-loading was regarded as negligible. The specifications of the walls of all the series are as indicated in Table 1.

The ultimate shear strength shown in Table 1 were calculated by (AIJ 1999) and (AIJ 2010) based on the truss and arch theory and shown in (Eq. (1).

$$V_u = t_w l_{wb} P_s \sigma_{sy} \cot\phi + \tan\theta(1-\beta) t_w l_{wa} \nu\sigma_B / 2 \tag{1}$$

$$\beta = \{(1+\cot^2\phi) P_s \sigma_{sy}\} / \nu\sigma_B, \quad \tan\theta = \sqrt{(h_w / l_{wa})^2 + 1} - h_w / l_{wa}$$

Where, t_w: Wall thickness (mm), l_{wa}, l_{wb}: Equivalent wall length(mm),

P_s: Shear reinforcement ratio of the wall, v: Effective compression strength coefficient,
σ_{sy}: Strength of the shear reinforcement of the wall, σ_B: Compressive strength of concrete,
ϕ: Angle of concrete compression strut of truss mechanism, h_w: Wall height(mm)

Table1 – Summary of specimens

	Name of specimen		SC-13 Series	SC-06 Series	SF-13 Series
	Damage class		0~Ⅳ（None～Severe)	0~Ⅳ（None～Severe)	0~Ⅳ（None～Severe)
Shear wall	Height(mm)		1000		
	Length (mm)		1800		
	Thickness (mm)		120		
	Arrangement of reinforcement		D6@40(SD295) Double	D6@80(SD295) Double	D6@40(SD295) Double
	Reinforcement ratio (%)		1.32	0.66	1.32
	Shear span to depth ratio		0.29		
Boundary confining conditions	Column	Section b×D (mm)	200×200		
		Main reinforcement	12-D16(SD345)		
		Hoop reinforcement	2-D10(SD345)@60		
	Flange wall	Height (mm)			1000
		Length (mm)			600
		Thickness (mm)			120
		Arrangement of reinforcement			D6@40(SD295) Double
		Reinforcement ratio (%)			1.32
Strength (kN) AIJ (1999)			Based on Materials properties		
Shear cracking strength (kN)			571	325	429
Ultimate shear strength (kN)			1697	1343	1504
Flexural cracking strength (kN)			356	323	535
Ultimate flexural strength (kN)			4453	3852	2810

Table-2 Material properties

Name of specimen	Concrete strength Fc (N/mm^2)	reinforcement	Yield strength (N/mm^2)	Ultimate tensile (N/mm^2)
SC-13-D0	40.2	D6(SD295)	348	518
		D10(SD345)	350	572
		D16(SD345)	352	518
SC-06-D0	32.1	D6(SD295)	388	541
		D10(SD345)	364	584
		D16(SD345)	397	570
SF-13-D0	30	D6(SD295)	367	530

2.2 Details of Specimens

Dimensions and reinforcement arrangement for the three experimental series is shown in Figure 1, for SC-13 Series, SC-06 Series and SF-13Series.SC-13 Series and SC-06 Series have columns in both sides of the wall, also base beams. While, SF-13Series have two flange walls at both ends of the wall. All the series specimens have a total height of 1800mm, wall with a height of 1000mm and a thickness of 120mm.

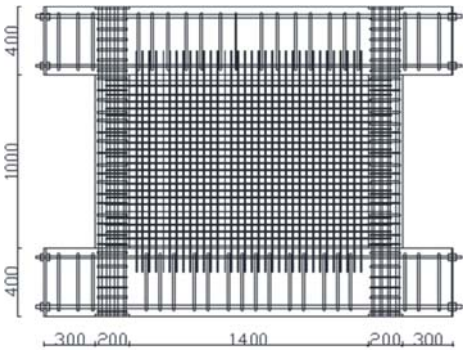

a) Series SC-13

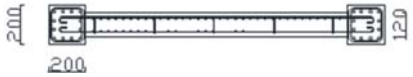

Column: Main reinforcement 12-D16(SD345)
Hoop reinforcement 2-D10(SD345) @60
Shear wall: D6@40(SD295) Double

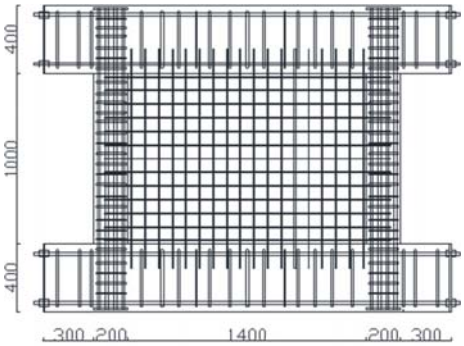

b) Series SC-06

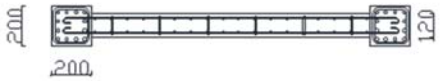

Column: Main reinforcement 12-D16(SD345)
Hoop reinforcement 2-D10(SD345) @60
Shear wall: D6@80 (SD295) Double

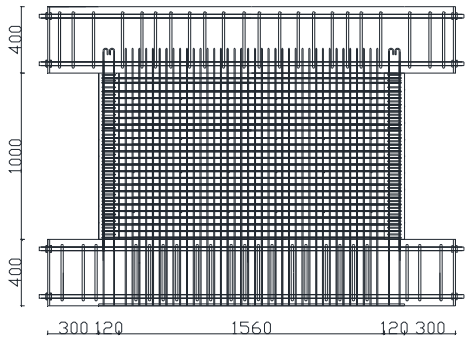

c) Series SF-13

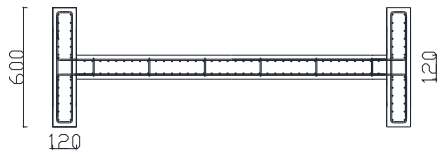

Flange wall: Arrangement of reinforcement
D6@40(SD295) Double

Shear wall: D6@40(SD295) Double

Figure 1 Dimension and reinforcing details of specimens: (units in mm)

2.3 Loading Plan

Loading setup is shown in Figure 2. Vertical loads are applied to the wall and columns by two vertical hydraulic jacks, to maintain a constant axial stress about 0.5MPa (total of 125kN applied by the two vertical jacks). Moreover, cyclic horizontal load is applied using two hydraulic jacks fixed at the mid-height of the wall, in order to make the inflection point at the mid-height of the specimen. As a result, the shear span ratio to depth of the wall is about 1/3. Loading procedures for all series, except for specimen D0, as illustrated in Figure 3, comprise of two main phases, the first is application of the pre-loading until the specimens reach a certain damage level similar to that observed after an earthquake. Then, the second phase, main loading is applied to all specimens until failure of specimens.

The loading cycles for specimens D0 (control specimen) in all the series consists of two cycles at each story drift until it reaches failure as shown in Table 2. The damage observed in the specimens D0 at each drift

angle is used as a reference, which is then used to decide the maximum drift angle used in the pre-loading phase. The maximum drift angles in pre-loading correspond to the target four damage levels: slight, minor, moderate and severe. The classification of damage level and details for pre-loading protocols for other specimens are discussed in the next section. After five cycles of loading at the target level, the specimen was unloaded by gradual cyclic loading and then the main-loading was conducted.

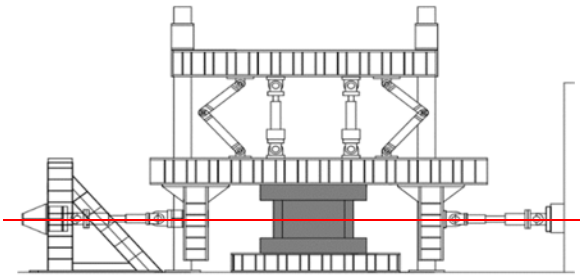

Figure 2 Loading test setup

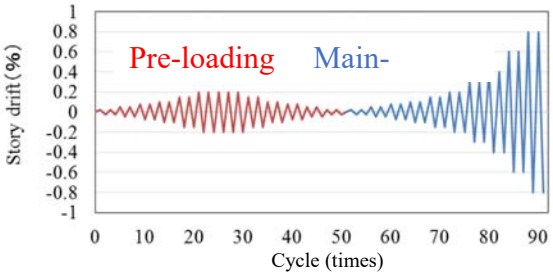

Figure 3 Loading history

Table 2 –Loading schedule: D0 (similar for all 3 series)

Loading type*	Specimens	Story Drift R(/1000rad.) and Number of Each Cycle *(no pre-load is applied to specimens D0)											
		±0.25	±0.5	±0.75	±1	±1.5	±2	±2.5	±3	±4	±6	±7	8
Main loading	SC-13-D0 SC-06-D0 SF-13-D0	2	2	2	2	2	2	2	2	2	2	2	2

3. Experimental results of the experiment: D0-of all series

3.1 Shear force-displacement relationship and failure behaviour of specimen

Shear force-story drift angle relationship of specimens D0 are shown in Figure 4.

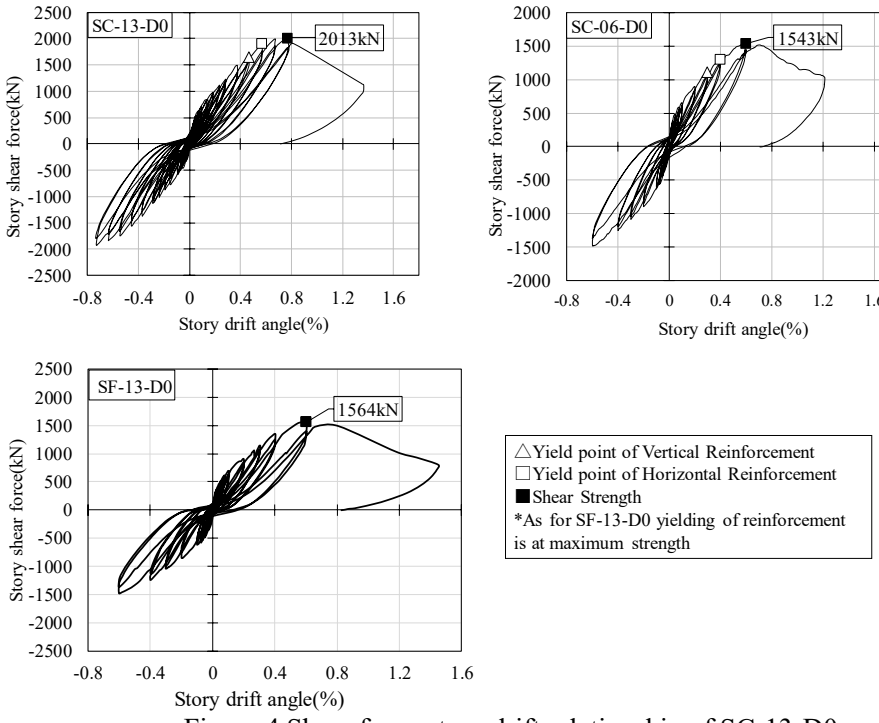

Figure 4 Shear force-story drift relationship of SC-13-D0

Cracks pattern and final damage states are shown in Figure 5**.** Note that recording of cracks is conducted on half side of the wall (left), since symmetrical damage pattern is assumed due to symmetrical stress distribution. Initial cracks in all specimens were observed at the corner of the wall panel at story drift of 0.025%. At the cycle of story drift 0.2%, cracks developed in the entire wall panel. As for specimen S-13-D0 and SF-13-D0, with relatively high reinforcement ratio *Ps*=1.3%, the crack interval was found to be close and of a value similar to that of reinforcement interval. Furthermore, the vertical reinforcement and horizontal reinforcement yielded at story drift of 0.3%~0.4% for specimen SC-06-D0, reinforcement ratio of *Ps*=0.66%, which is relatively at earlier drift than of SF-13-D0, which yielded at 0.5%~0.6%.
The maximum shear force was reach as story drift of 0.8% for Specimen SC-13-D0, and at story drift 0.6% for specimen SC-06-D0 and SF-13-D0. The shear force reached the maximum value with concrete spalling, and then rapid drop of shear strength and crushing of concrete had occurred.

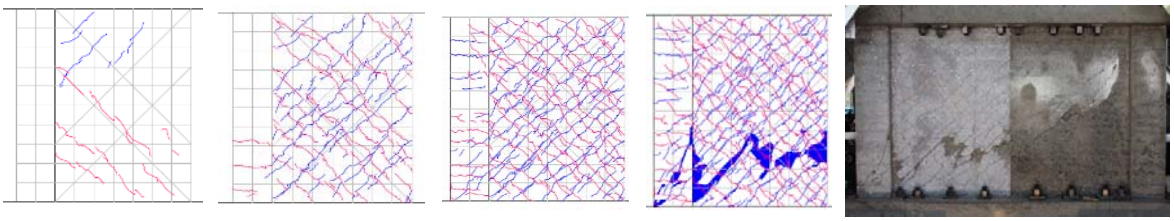

a) SC-13-D0

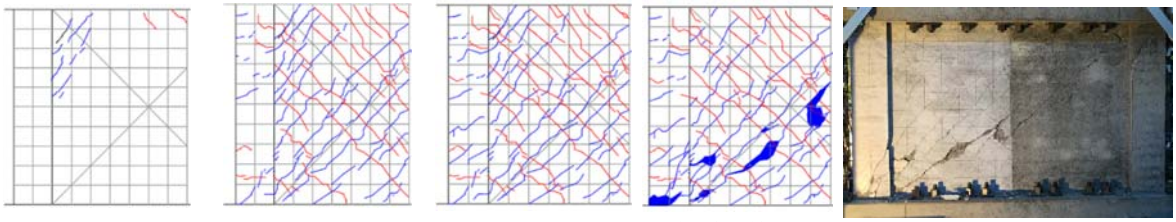

b) SC-06-D0

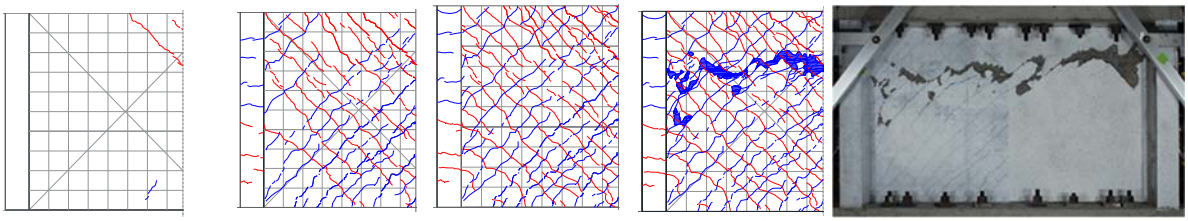

c) SF-13-D0

Figure 5 Cracking patterns of SC-13-D0, SC-06-D0, SF-13-D0

3.2 Classification of Damage Class in Specimen S-D0 in all series

Japan Guideline (JBDPA 2015), originally issued in 1990, was revised in 2001 and 2015. In this Guideline, damage classes of structural elements are classified into five classes according to Table 3 and Figure 6, based on the damage situation such as the maximum residual crack width, spalling of concrete, and buckling or fracture of steel bars. In this paper, damage classes in the shear walls (S-13-D0, S-06-D0 and SF-13-D0) are judged based on the Post-Earthquake Damage Evaluation Guideline. In addition, the load-deflection curve, stiffness degrading ratio and yielding states of the reinforcement as well as the crack width are considered to determine those damage classes and their corresponding story drift.

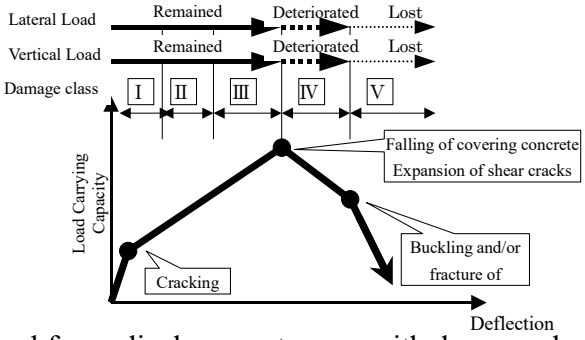

Figure 6 Idealized lateral force-displacement curve with damage class based on (JBDPA 2015)

Table 3 Damage classes of structural elements from Japanese damage evaluation (JBDPA 2015)

Damage class	Damage situation
I	Some cracks are found. Crack width is smaller than 0.2 mm.
II	Cracks of 0.2 - 1 mm wide are found.
III	Heavy cracks of 1 - 2 mm wide are found. Some spalling of concrete is observed.
IV	Many heavy cracks are found. Crack width is larger than 2 mm. Reinforcing bars are exposed due to spalling of the cover concrete.
V	Buckling of reinforcement, crushing of concrete and vertical deformation of columns and/or shear walls are found. Side-sway, subsidence of upper floors, and/or fracture of reinforcing bars

As a result, the damage class I corresponding to the cracking drift is found to be less than 0.1%, the drift of 0.1%~0.3% corresponds for damage class II, and the drift of 0.3%~0.5% is for damage class III, and the drift of 5/1000rad~ultimate shear strength is determined as the damage class IV, as shown in Figure 7. Thus, pre-loadings protocols for specimens S-DI~IV were carried out, as shown in Table 4.

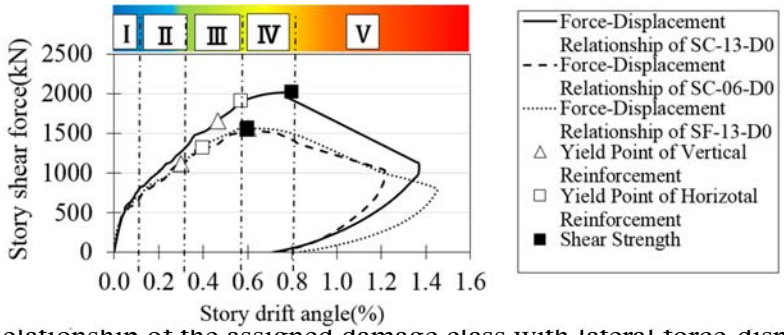

Figure 7 Relationship of the assigned damage class with lateral force-displacement

Table 4– Loading schedule of damaged specimens: DI~DIV (All of Series)

	Pre-Loading													
	Story Drift R(/1000rad.) and Number of Each Cycle (Time)													
Specimens	±0.25	±0.5	±0.75	±1	±2	±3	±4	±6	±4	±3	±2	±1	±0.5	±0.25
DI	2	5	5										2	2
DII	2	2	2	2	5							2	2	2
DIII	2	2	2	2	2	2	5			2	2	2	2	2
DIV	2	2	2	2	2	2	2	5	2	2	2	2	2	2

	Main Loading										
	Story Drift R(/1000rad.) and Number of Each Cycle (Time)										
Specimens	±0.25	±0.5	±0.75	±1	±1.5	±2	±2.5	±3	±4	±6	Final
DI~DIV	2	2	2	2	2	2	2	2	2	2	2

4. Experimental results of the experiment: DI ~ DIV-of all series

4.1 Shear force-story drift angle relationship of damaged specimen

Shear force-story drift angle relationship in the positive loading of all the pre-damaged specimens (DI ~ DIV) for all the series is shown in Figure 8. All the specimens showed similar behaviour to the behaviour of specimen D0 with no pre-damage of each series. It should be noted, that for specimens SC-13-DII, SC-06-DII and SF-13-DI, the loading was not carried out until the ultimate damage phase, and they were reused as specimens SC-13-DIV, SC-06- DIV and SF-13-DIV, respectively. This is because the thought was, for this specimens, pre-damage will not affect the behaviour comparing to the undamaged specimen.

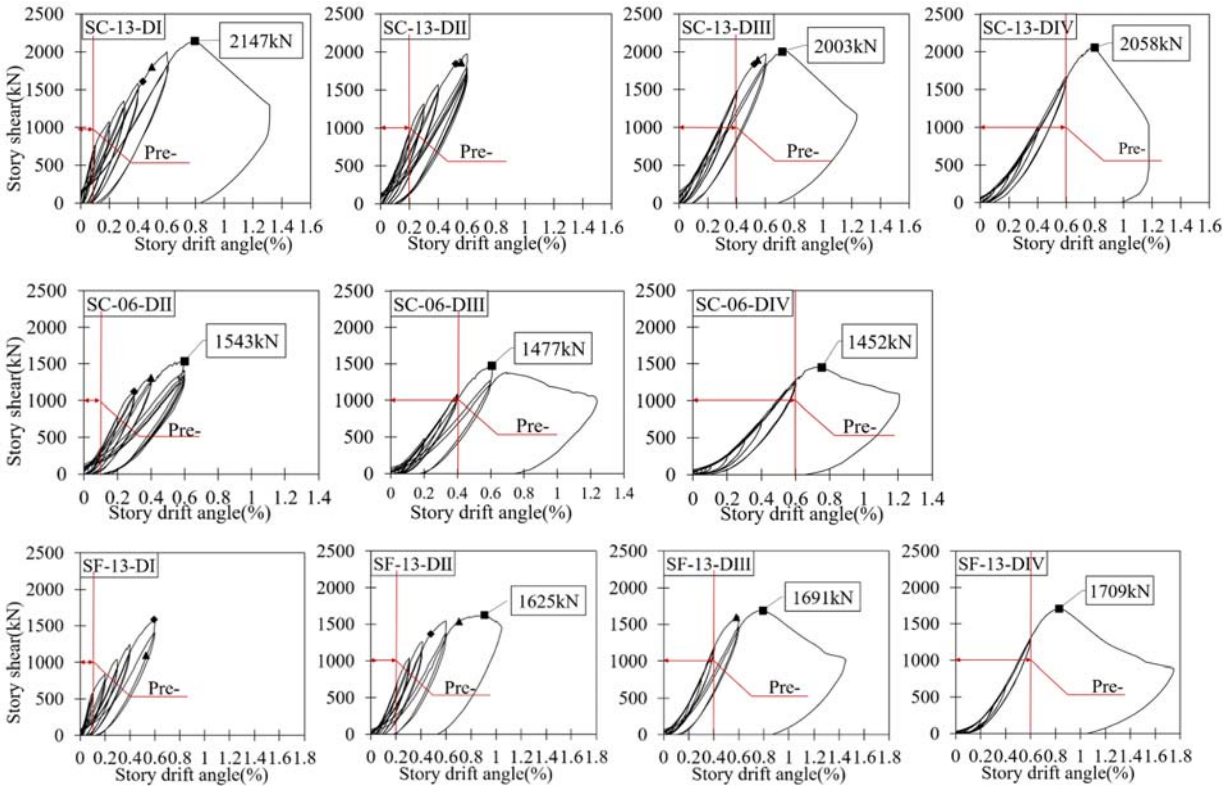

Figure 8 Shear force-story drift angle relationship of damaged specimens

4.2 Comparison of stiffness degradation.

The relationship between story drift and stiffness degrading is illustrated in Figure 9. The stiffness of all of the pre-damaged specimens in each series are compared to the initial stiffness of the same specimen at the pre-loading phase. The initial stiffness is calculated based on the initial loop of 0.025% Cycle. While for the rest of the cycles, stiffness is calculated based on the slope of the line connecting the positive and negative peak point at each cycle. It is noticed that even for damage class I that experienced small deformation and limited damage during the pre-damage phase, the initial stiffness decreased to around half for D0 specimen. It can also be noticed that the equivalent stiffness deceases as the pre-damage level increases. On the other hand, beyond experienced deformation in the pre-loading phase almost no difference is noticed in stiffness compared to the undamaged specimen D0 in each series.

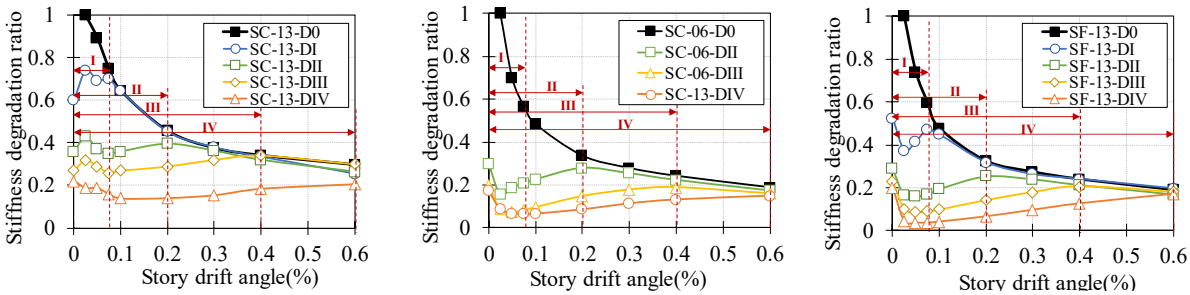

Figure 9 stiffness degrading ratio

4.3 Comparison of shear strength and deformation capacity

Envelopes of the shear force – story drift for all the specimens in each series are demonstrated in Figure 10. In every curve of each damaged specimen, it is noticed that the capacity of the wall is less than that for the undamaged specimen D0, and that is attributed to the degradation of equivalent stiffness as shown in Figure 9. However, beyond the point of story drift which represent the pre-loading limit for each damaged specimen almost no difference at capacity is noticed compared when compared to the specimens D0 of series SC-13 and SF-13 (specimens with relatively high reinforcement ratio) as shown in Figure 11. On the other hand, in S-06 series, the maximum shear force of the specimens with damage level III or IV at their main loadings showed a slight reduction value of about 10% but this observation is not conclusive since the number of specimens is limited. The results showed that no significant deterioration was observed in ultimate strength and maximum deformation capacity due to previous damage.

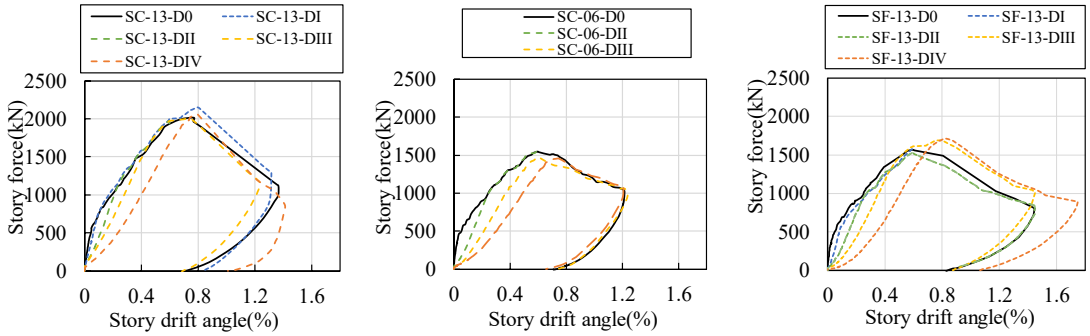

Figure 10 envelope of shear force – story drift curves for different damage level

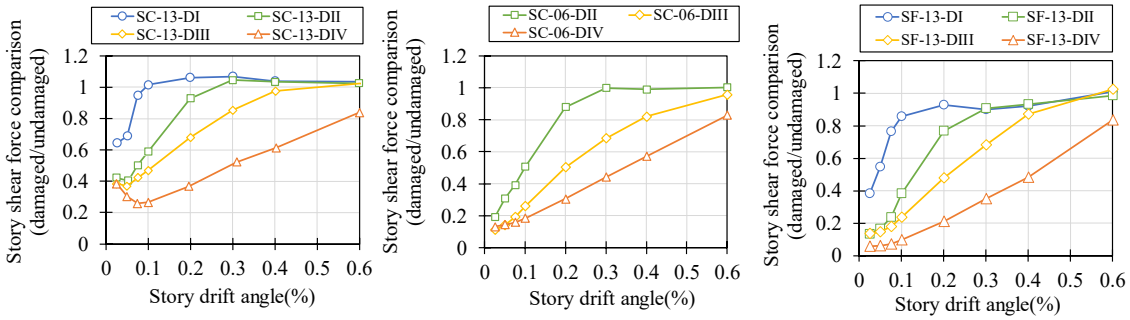

Figure 11 Lateral force at each drift of the damaged specimens compared to the undamaged specimen

4.4 Comparison of energy dissipation capacity

Envelopes Energy absorption of one cycle is indicated by the loop area. The degradation of energy absorption capacity could be judged by the ratio of loop area of damaged specimen to the loop area of specimen without pre-damage (D0). The changes of loop area ratio are shown in Figure 12. In SC-13 series and SC-06 series, at the small story drift angle, the energy absorbing capacity of pre-damaged specimens was degraded by 40~80% according to the damage levels. However, when the story drift of the wall is in unexperienced area, the energy dissipation capacity of pre-damaged specimens in SC-13 series is equal to that of no-pre-damaged one, that is, the loop area ratio is nearly equal to 1.0. Specimens in series SF-13, with boundary element as flange wall, showed relatively more degradation in loop area than other series.

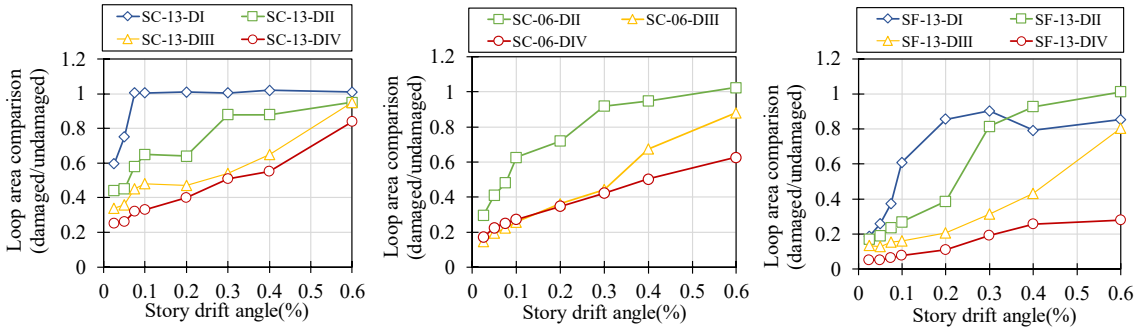

Figure 12 Ratio of loop area at each cycle of the pre-damaged specimens to the control specimen D0

CONCLUSION

Three series of tests of 1\4 scale reinforced concrete (RC) shear wall using static cyclic loading were conducted. The investigated parameters are: two levels of wall reinforcement ratio, column and flanged boundary of shear walls and four levels of initial damage. The specimens were designed to failed in shear to represent a concrete shear walls in reactor buildings. The objective of tests is to clarify the influence of prior damage to seismic capacity of shear walls based on influence of prior damage.

The results showed that no significant deterioration was observed in ultimate strength and maximum deformation capacity due to previous damage. Specimens with flange boundaries have relatively greater stiffness degradation and smaller energy dissipation. The specimens with walls of less reinforcing ratios showed a slight degradation of strength of less than 10 % when subjected to prior damage level IV (Severe damage), but those results are inconclusive due to limited number of specimens. The relationship between prior damage level and observed degradation of stiffness is obtained which is useful in remodelling of RC walls using modified backbone curve.

REFERENCES

Architectural Institute of Japan (AIJ). (1999). “Design Guidelines for Earthquake Resistant Reinforced Concrete Building Based Inelastic Displacement Concept” (in Japanese)

Architectural Institute of Japan (AIJ). (2010). “AIJ Standard for Structural Calculation of Reinforced Concrete Structures”)in Japanese

Japan Building Disaster Prevention Association (JBDPA). (2001). “Standard for Post-Earthquake Damage Level Classification of Reinforced Concrete Building”

Kai J. Marder, Christopher J. Motter, Kenneth J. Elwood, G. Charles Clifton (2018) “ Effects of variation in loading protocol on the strength and deformation capacity of ductile reinforced concrete beams” Earthquake Engng Struct Dyn. 2018;47:2195–2213

Pujol S, Sozen MA, Ramirez JA. (2006). Displacement history effects on drift capacity of reinforced concrete columns. ACI Struct J. 2006;103(2):253.